Journal of Intelligent & Robotic Systems (2024) 110:33
https://doi.org/10.1007/s10846-024-02066-7

REGULAR PAPER

Control of the PVTOL with Strong Input Coupling

Rogelio Lozano[1,2] · Jhonatan F Eulopa-Hernandez[1] · Sergio Salazar-Cruz[1]

Received: 1 June 2023 / Accepted: 23 January 2024 / Published online: 15 February 2024

Abstract
This paper studies the modeling and control of a Planar Vertical Take-Off and Landing (PVTOL) with steerable thruster. A longitudinal model is obtained using Newton's second law for the PVTOL which evolves in 3 degrees of freedom and has two control inputs. The aerial vehicle is driven by steerable propulsion controlling its evolution in the vertical plane through the thrust and torque control inputs, which drive the vehicle body and generate a rotation. The obtained model is nonlinear and is significantly different with respect to the well-known PVTOL. For this reason, different control algorithms are presented, and the closed-loop behavior is studied for each of them. The proposed control strategies perform a stationary flight at a desired altitude and control the position of the aerial vehicle. The performance of the proposed control algorithms is tested in numerical simulations.

Keywords Thrust vector control · Linear feedback control · Stationary flight · Closed-loop system

1 Introduction

The PVTOL has drawn the interest of many researchers because it is a nonlinear dynamical system that simulates the longitudinal dynamics of a helicopter or multirotor UAV (Unmanned Aerial Vehicle). It only has two control inputs while having three degrees of freedom.

In an ideal scenario, the vertical and horizontal accelerations of the vehicle are proportional to the projections of the thrust vector and the angular acceleration is proportional the torque. Implicitly, there is a decoupling of the inputs, as the thrust only influences linear accelerations and the torque input only impacts rotational acceleration. In the literature, many PVTOL control methods have been suggested.

Hauser et al. [1] introduced one of the first controllers that were suggested for the PVTOL. They demonstrated that when the PVTOL's flight control is subjected to an accurate input-output linearization approach, the resulting system exhibits unstable internal dynamics. They put forth a solution using a rough input-output linearization technique designed for nonlinear systems with somewhat non-minimal phase.

A nested saturation control was suggested in [2] to stabilize the PVTOL. The stability was guaranteed only when the orientation angle θ and its derivative were initially sufficiently small. The idea to employ nested saturation arose from the observation that when the altitude is controlled by nonlinear compensation, the resulting subsystem from the torque input τ to the output x (the horizontal displacement) reduces to four integrators in cascade when θ is small, i.e., when $\tan\theta \approx \theta$.

Brandão et al. [3], in contrast, suggests a nonlinear controller based on Lyapunov Theory to stabilize a quadrotor to execute positioning and trajectory tracking tasks constrained to a vertical plane. Due to flying restrictions motion limited to the XZ and YZ planes. The maneuvers described are frequently carried out using PVTOL vehicles. A nonlinear controller is proposed and the closed-loop system stability is proved. To prevent the physical actuators from becoming saturated, the proposed controller includes saturating the control signals.

A controller based on a PD controller and a sliding mode controller was published in [4] to stabilize both the horizontal and angular variables to the desired rest position. It was

✉ Sergio Salazar-Cruz
sesalazar@cinvestav.mx

Rogelio Lozano
rogelio.lozano@cinvestav.mx

Jhonatan F Eulopa-Hernandez
jhonatan.eulopa@cinvestav.mx

[1] LANAVEX, CINVESTAV, Av. IPN, CDMX 07360, CDMX, México

[2] Université de technologie de Compiégne, Heudiasyc CNRS, Compiégne 60319, France

established that the closed loop system is locally stable if the initial angular rate and angular position fall inside a certain area without any singularities.

In [5], a hierarchical control approach was suggested for a small VTOL vehicle to monitor a desired trajectory. By employing this orientation angle as a virtual input to maintain the aircraft location, their control approach gets around the topological restriction on the orientation.

Additionally, a control strategy to provide a globally stable controller for UAVs was suggested in [6]. They also have an adaptive control method that can deal with unknown system parameters.

A robust controller was suggested in [7] to solve the PVTOL aircraft trajectory tracking control problem under crosswind. The controller combines active disturbance rejection control and input-output feedback linearization algorithms. The latter reduces the impacts of crosswinds, while the former linearizes the PVTOL dynamics.

In [8], a control approach for the well-known PVTOL problem was provided. To achieve the target height, the total force is calculated using nonlinear feedback compensation. The orientation angle is then selected as a smooth saturation function of $x, \dot{x}$, controlling the horizontal position x. The Lyapunov approach was used to obtain a stability proof.

Lozano et al. [9] shows how the nested saturation control may be improved by choosing specific values of the saturation amplitudes. The proposed controller is proved to be globally stable.

It is worth highlighting that in the case of an ideal PVTOL, the thrust only provides linear accelerations and the torque produces only rotational acceleration. Nevertheless, when the PVTOL thrusters are not perfectly aligned, the torque produces also a small translational acceleration. This situation is referred to as the PVTOL issue with strong coupling at the inputs. Due to its difficulty, there are only few control techniques that have been proposed in the literature as described below.

The global stabilization of the VTOL aircraft with strong coupling at the inputs was addressed in [10] using uniform static state feedback. Furthermore, applying a decoupling coordinate change results in the generation of differentially flat outputs for VTOL aircraft.

On the other hand, [11] proposed an ideal control based method for examining feasible nonlinear system trajectories. It serves as a prototype tool for tracking trajectories in the presence of constraints. The approach is based on new optimization approaches for optimum control problems with pointwise constraints applied to a PVTOL, dynamic embedding, and constraint relaxation.

Similarly, [12] proposed an ideal trajectory planner for spacecraft orientation control subject to input saturation and angular velocity restrictions. It handles the nonlinearity of the variety of unit quaternions by adapting Newton's approach for trajectory optimization. A modified interior point technique is then used to manage the system limitations so that it may still be used in cases when an intermediate solution estimate is not practical.

The well-known PVTOL has two thrusters attached by a bar and the center of gravity is located in the middle of the bar. The present paper deals with an aerial vehicle evolving in a vertical plane that is driven by a single thruster. The thruster can be oriented with respect to the body of the aircraft. Therefore, the two control inputs are the thrust magnitude and the angle between the thruster and the body of the aircraft. However, the center of mass is located in the body of the aircraft. This means that in a hover flight, the orientable thruster is located at certain distance below the center of gravity.

Several aerial vehicles belong to this category. Tail sitter airplanes take-off and land vertically and its orientation is controlled using the control surfaces of the tail (elevon and rudder) which deviate the airflow generated by the rotors. VTOL airplanes like Wingtra belong also to this category. VTOL jet fighters can also take-off vertically using a vectored thrust engine in the middle of the fuselage which is used to control the orientation of the aircraft. Some rockets have a single thruster which can be tilted. These are also called vectored or steerable thrusters and are used to control the orientation of the rocket to perform precise take-off and landing or hover. There exist also small electric rockets which are driven by two counter-rotating rotors which can be rotated and therefore operate as a vectorized thruster. The aircrafts mentioned above are presented in Fig. 1.

A PVTOL aircraft can intuitively be controlled by adjusting the total thrust to control the altitude and then use independently the torque to control the aircraft orientation to move forward or backward. In the case of a rocket with vectorized thrust the torque is generated by changing the orientation of the thruster which is situated at a certain distance from the center of gravity. Therefore, if we aim to move the aircraft forward we tilt the thruster in the opposite direction so that the orientation of the rocket tilts forward. Notice however that the rocket first moves backward before moving forward. This is a typical characteristic of non-minimum phase systems. Notice also that in the PVTOL dynamical equation the torque input appears only in the equation of the angular accelerations. Meanwhile in the case of a rocket (or any aircraft driven by a vectorized thrust) the torque appears also in the equations for the vertical and horizontal accelerations and thus requires the synthesis of a specific control strategy.

The present paper studies a PVTOL with steerable propulsion and the control objective is to perform a stable hover flight. The dynamical model of the aerial vehicle driven by a vectored thruster is very different to the classical PVTOL model. Three control strategies for such a PVTOL model with strong input coupling are proposed. The closed-loop

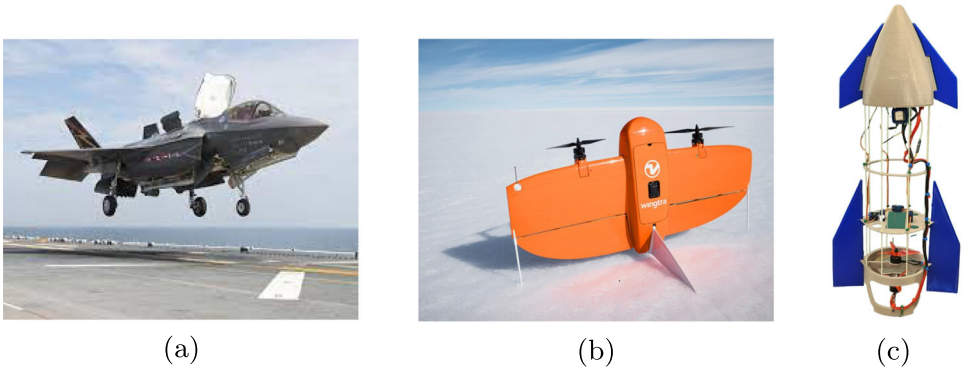

Fig. 1 (a) VTOL jet fighter, (b) Tail sitter VTOL Drone, (c) Electric rockets

system behavior of the proposed control laws is analyzed, and a comparative study is presented. The objective is to control the longitudinal model of the aircraft using simple control laws to perform a stationary hover flight at a desired altitude and position. The performance of the proposed controllers is tested in numerical simulations.

This paper is organized as follows. Section 2 describes the PVTOL aircraft with strong input coupling and presents the dynamical model. Section 3 presents three different control algorithms and their performance in numerical simulation. The results obtained in numerical simulation are analyzed in Section 4. Finally, conclusions are given in Section 5.

2 Model of the PVTOL with Strong Input Coupling

This section describes the model of the PVTOL in the vertical plane with strong input coupling. For simplicity we describe the model in a simplified rocket as shown in Fig. 2. Let θ be the angle of the rocket with respect to the vertical, g be the force of gravity, m be the mass of the rocket, C be the center of gravity of the rocket located in the middle of its fuselage, l be the mean distance and F be the thrust force of the rocket engine.

From Fig. 2, we obtain the equations of the dynamic model for the rocket system using the second law of Newton, which are as follows.

$$I\ddot{\theta} = \tau \tag{1}$$

$$\ddot{x} = f\sin\theta - \frac{\tau}{l}\cos\theta \tag{2}$$

$$\ddot{y} = f\cos\theta + \frac{\tau}{l}\sin\theta - mg \tag{3}$$

where

$$\tau = lf_T \tag{4}$$

$$f_T = F\sin\gamma \tag{5}$$

$$f = F\cos\gamma \tag{6}$$

where γ is the angular displacement of the thruster with respect to the fuselage, F is the total thrust of the rocket and is decomposed into the forces f and f_T.

Note also that

$$\tan\gamma = \frac{f_T}{f} \tag{7}$$

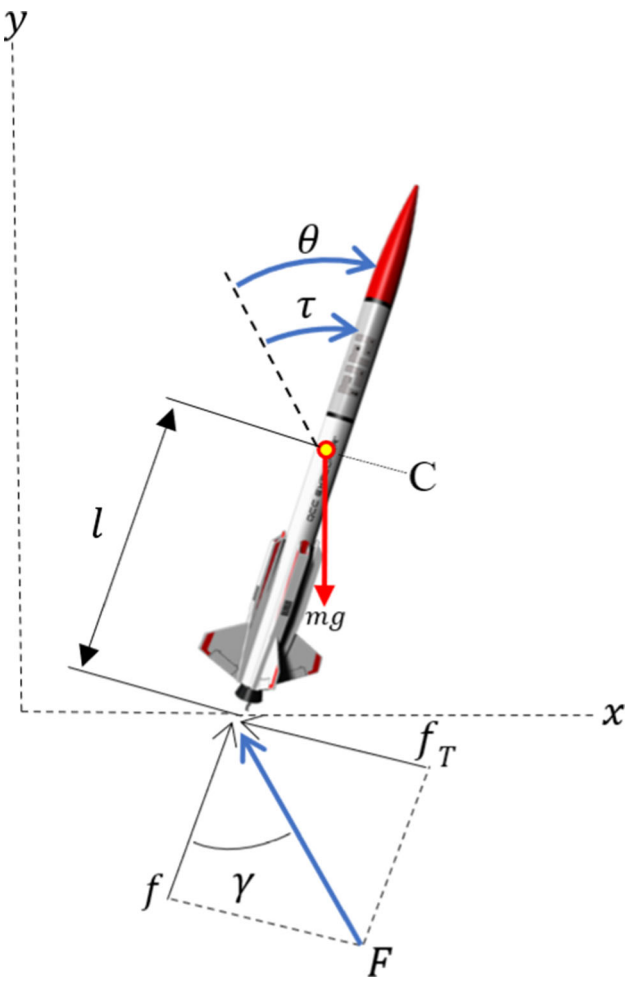

Fig. 2 Forces acting on the simplified rocket. F is the total thrust of the rocket which is decomposed into the forces f and f_T

$$F = \sqrt{f^2 + f_T^2} \tag{8}$$

In the following sections control algorithms will be proposed for the model given in Eqs. 1, 2 and 3.

Assumption 1. To simplify the presentation of the 3 control algorithms it is assumed that $I = 1, l = 1$.

2.1 Control Algorithm 1

This algorithm is based on a change of the control variables that partially linearizes the system.

Consider the following equations describing the rocket's operation which using Assumption 1 can be rewritten as

$$\ddot{\theta} = \tau \tag{9}$$

$$\ddot{x} = f \sin\theta - \tau \cos\theta \tag{10}$$

$$\ddot{y} = f \cos\theta + \tau \sin\theta - mg \tag{11}$$

New input variables are defined as u_1, u_2

$$\begin{bmatrix} u_1 \\ u_2 \end{bmatrix} = \begin{bmatrix} \sin\theta & -\cos\theta \\ \cos\theta & \sin\theta \end{bmatrix} \begin{bmatrix} f \\ \tau \end{bmatrix} \tag{12}$$

Introducing Eq. 12 Eqs. into 9, 10 and 11 we obtain

$$\ddot{\theta} = \tau \tag{13}$$

$$\ddot{x} = u_1 \tag{14}$$

$$\ddot{y} = u_2 - mg \tag{15}$$

Once the virtual control inputs u_1, u_2 are obtained, the original inputs f, τ can be calculated from Eq. 12 as follows

$$\begin{bmatrix} f \\ \tau \end{bmatrix} = \begin{bmatrix} \sin\theta & \cos\theta \\ -\cos\theta & \sin\theta \end{bmatrix} \begin{bmatrix} u_1 \\ u_2 \end{bmatrix} \tag{16}$$

We propose u_2 as follows to control the altitude, so that y converges to a desired altitude y_d.

$$u_2 = -2\dot{y} - (y - y_d) + mg \tag{17}$$

Introducing Eq. 17 into Eq. 15 gives a closed-loop system

$$\ddot{y} + 2\dot{y} + (y - y_d) = 0 \tag{18}$$

From the above, it is concluded that $y \to y_d$, $\dot{y} \to 0$, $u_2 \to mg$.

Then Eqs. 13 and 14 can be written as

$$\ddot{\theta} = -\cos\theta u_1 + \sin\theta u_2 \tag{19}$$

$$\ddot{x} = u_1 \tag{20}$$

Assuming that θ is near the origin, the above equations are approximated by

$$\ddot{\theta} = -u_1 + \theta mg \tag{21}$$

$$\ddot{x} = u_1 \tag{22}$$

To control the state of the above linear system, we propose the state feedback control input u_1 as follows

$$u_1 = k_1\theta + k_2\dot{\theta} + k_3 x + k_4\dot{x} \tag{23}$$

Introducing Eq. 23 into Eqs. 21 and 22 and applying the Laplace transform

$$\underbrace{\begin{bmatrix} s^2 + k_1 + k_2 s - mg & k_3 + k_4 s \\ -k_1 - k_2 s & s^2 - k_3 - k_4 s \end{bmatrix}}_{A_{CL}} \begin{bmatrix} \theta \\ x \end{bmatrix} = 0 \tag{24}$$

Calculating the determinant of A_{CL} gives

$$det\, A_{CL} = s^4 + s^3(k_2 - k_4) + s^2(k_1 - k_3 - 1) + sk_4 + k_3 \tag{25}$$

The closed loop system poles can be selected arbitrarily as long as they belong to the stable region. In the numerical simulation the proposed closed loop control system has been chosen to have 4 poles at -1. Therefore the characteristic polynomial of the closed loop system is:

$$(s+1)^4 = s^4 + 4s^3 + 6s^2 + 4s + 1 \tag{26}$$

Assuming that $mg = 1$, the gains are as follows

$$k_1 = 8 \tag{27}$$

$$k_2 = 8 \tag{28}$$

$$k_3 = 1 \tag{29}$$

$$k_4 = 4 \tag{30}$$

Substituting the above gains into Eq. 23 gives the following state feedback law

$$u_1 = 8\theta + 8\dot{\theta} + x + 4\dot{x} \tag{31}$$

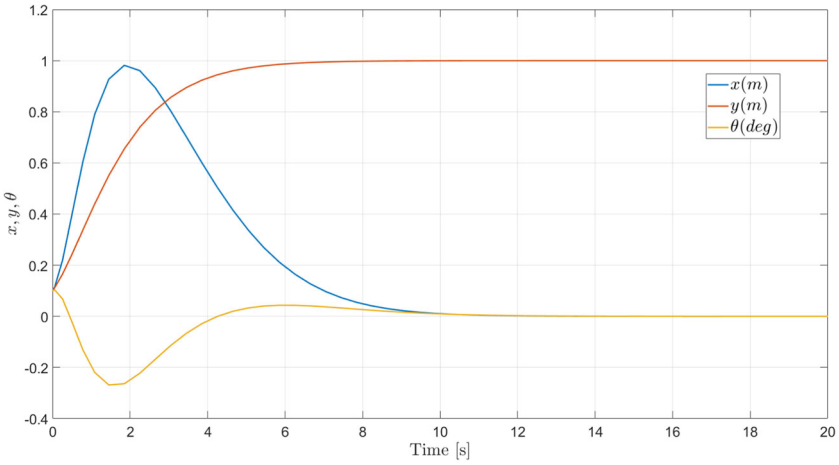

Fig. 3 Evolution of states x, y, θ

From the above we conclude that the subsystem state Eqs. 21 and 22 i.e. $[x, \dot{x}, \theta, \dot{\theta}]$ converges to the origin. Since we assumed that θ is in a neighborhood of the origin then the convergence to the origin is local.

2.1.1 Simulation of the Proposed Control Algorithm 1

Figure 3 presents the evolution of x, y, θ and Fig. 4 presents the evolution of τ, f under the following initial conditions; $\dot{\theta}(0) = 0.12$, $\theta(0) = 0.1$, $\dot{y}(0) = 0.2$, $y(0) = 0.1$, $\dot{x}(0) = 0.2$, $x(0) = 0.1$, $y_d = 1$. It can be observed in Figs. 3 and 4 that x and θ converge both to zero while y converge to the desired output.

2.2 Control Algorithm 2

This section presents a control algorithm which is based on the following strategy. The control input f is proposed in such a way that equation Eq. 11 is linearized assuming that $\tau \sin\theta$ is small. Then the control input τ is proposed in Eq. 9 so that θ will track the sum of two saturation functions which depend on x and $\dot{x}$. The amplitudes of such saturation functions are chosen small enough to satisfy that $\tau \sin\theta$ is small. Then the right hand side of Eq. 10 becomes approximately equal to the sum of the saturation functions and it can be proved that x converges to zero.

Consider the plant equations in Eqs. 9, 10 and 11. Suppose f is used to control the altitude, then

$$f = \frac{-2\dot{y} - y + y_d + mg}{\cos\theta} \tag{32}$$

By introducing the above equation into Eq. 11, it follows

$$\ddot{y} + 2\dot{y} + (y - y_d) = \tau \sin\theta \tag{33}$$

this means that if the term $\tau \sin\theta$ is small then $y \to y_d$, $\dot{y} \to 0$.

To control the subsystem Eq. 9 and 10 the following control law is proposed for τ.

$$\tau = -\theta - 10\dot{\theta} - \frac{1}{mg}(\sigma_a(\dot{x} + x) + \sigma_b(\dot{x})) \tag{34}$$

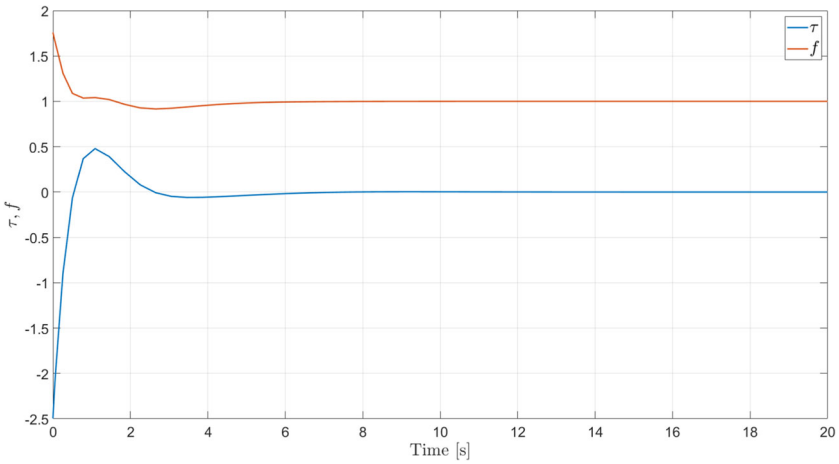

Fig. 4 Control inputs τ, f

The values of the parameters above have been tuned through simulations to give a reasonable transient. The obtained rise time, settling time and overshoot are given in Table 1.

The saturation function is defined as follows

$$\sigma_a(\chi) = \begin{cases} a & si \quad \chi > a \\ \chi & si \quad -a \leq \chi \leq a \\ a & si \quad \chi < -a \end{cases} \tag{35}$$

Introducing Eq. 34 into Eq. 9 gives the following closed loop

$$\ddot{\theta} + 10\dot{\theta} + \theta = -\frac{1}{mg}(\sigma_a(\dot{x} + x) + \sigma_b(\dot{x})) \tag{36}$$

The limits a, b of the two saturations are selected through simulation. They are selected as $a = 0.1$ and $b = 1.0$ such that after a certain time $|\theta| < \epsilon$, where $\epsilon = a + b$ is a small number and represents the upper bound on $|\theta|$. The damping coefficient 10 is selected such that $|\theta| < \epsilon$, in a short time. Then after a short time lapse one will have that the term $\tau \sin\theta$ in Eq. 33 is of order ϵ, so $y - y_d$ is of order ϵ too.

Considering that τ and θ are small, we have that $\tau \cos\theta \approx 0$, $f \approx mg$, $\sin\theta \approx \theta$. Then from Eq. 36 it follows that θ tracks the expression on the right-hand side of Eq. 36. It is concluded that Eq. 10 is approximately equal to the following equation.

$$\ddot{x} = -\sigma_a(\dot{x} + x) - \sigma_b(\dot{x}) \tag{37}$$

We have chosen $a = 0.1$ and $b = 1.0$ such that $a << b$. Define $V = \frac{1}{2}\dot{x}^2$. Then $\dot{V} = \dot{x}(-\sigma_a(\dot{x} + x)) - \sigma_b(\dot{x}))$. So when $|\dot{x}| > b$ it follows that $\dot{V} < 0$. Therefore after a finite time $|\dot{x}| < b$.

The above equation reduces to

$$\ddot{x} + \dot{x} = -\sigma_a(\dot{x} + x) \tag{38}$$

From the above it follows that $\dot{x} + x \to 0$ and then $x \to 0$

Table 1 Parameters of the behavior observed in simulations for the controllers

Algorithm 1			
	x	y	θ
Rise time	1.16	3.52	1.26
Settling Time	10.26	7.58	10.79
Steady state error	1.8 x 10^{-6}	0	1.17 x 10^{-5}
Algorithm 2			
	x	y	θ
Rise time	24.09	3.87	0.061
Settling Time	384.66	10.93	78.69
Steady state error	0.75	0	-2.55 x 10^{-2}
Algorithm 3			
	x	y	θ
Rise time	24.086	3.87	0.05
Settling Time	690.73	9.06	77.25
Steady state error	9.57 x 10^{-8}	0	-9.49 x 10^{-6}

2.2.1 Simulation of the Proposed Control Algorithm 2

Figure 5 presents the evolution of x, y, θ and Fig. 6 presents the evolution of τ, f under the following initial conditions; $\dot{\theta}(0) = 0.5$, $\theta(0) = 0.1$, $\dot{y}(0) = 0.02$, $y(0) = 0.03$, $\dot{x}(0) = 0.1$, $x(0) = 0.4$, $y_d = 20$. From Fig. 5 it follows that θ converge to zero, y converges to its desired value and x oscillates around zero. From Fig. 6 it follows that the inputs τ and f converge both to zero.

2.3 Control Algorithm 3

The control algorithm to be proposed in this section is also based on the altitude control using the control variable f and a stabilization of the variable θ using a single saturation function. This allows θ to converge to a neighborhood of the origin. Subsequently, the saturation function is selected such that the displacement x converges to the origin.

Let us consider again the system equations

$$\ddot{\theta} = \tau \tag{39}$$

$$\ddot{x} = f \sin\theta - \tau \cos\theta \tag{40}$$

$$\ddot{y} = f \cos\theta + \tau \sin\theta - mg \tag{41}$$

We propose again the control input f as

$$f = \frac{-2\dot{y} - y + y_d + mg}{\cos\theta} \tag{42}$$

and the control input τ as

$$\tau = -\theta - 10\dot{\theta} - \frac{1}{mg}\sigma_c(0.01x + \dot{x}) \tag{43}$$

In the above equation the control input τ has only one saturation function. The damping term fixed as 10 multiplying $\dot{\theta}$ modifies the speed of convergence. The proportional term fixed as 1 multiplying θ modifies the amplitude and finally the coefficient 0.01 multiplying x will reduce the influence of the initial condition $x(0)$ and therefore the control algorithm will first reduce the horizontal velocity $|\dot{x}|$ and once the velocity is small then the displacement x will converge to zero. Introducing Eq. 42 into Eq. 41 gives the following closed-loop system

$$\ddot{y} + 2\dot{y} + (y - y_d) = \tau \sin\theta \tag{44}$$

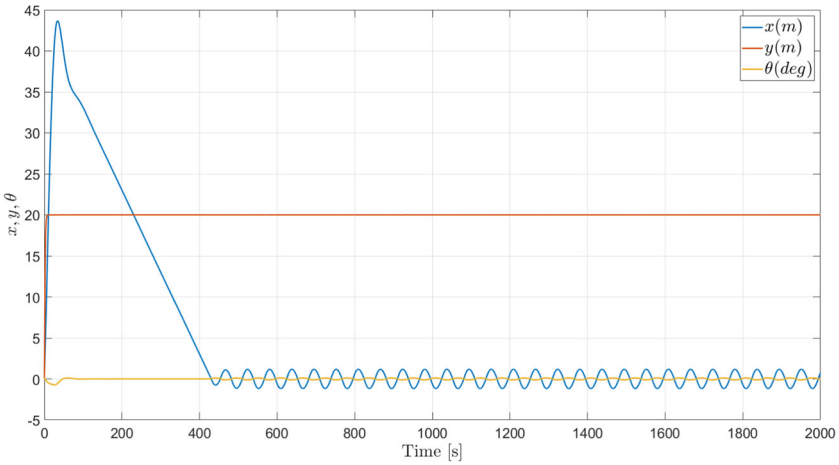

Fig. 5 Evolution of states x, y, θ

Introducing (43) into (39) we have

$$\ddot{\theta} + 10\dot{\theta} + \theta = -\frac{1}{mg}\sigma_c(0.01x + \dot{x}) \tag{45}$$

If the limit c in Eq. 43 is such that $c < \epsilon$ then after a certain time it will follow $|\theta| < \frac{\epsilon}{mg}$. Then from Eq. 43 it follows that $|\tau| < \frac{\epsilon}{mg}$ and after a certain time the term $\tau \sin\theta$ will be of the order of $(\frac{\epsilon}{mg})^2$.

For this reason, it is considered that τ and θ are small and it follows that $\tau \cos\theta \approx 0$, $f \approx mg$, $\sin\theta \approx \theta$. Then θ converges to the expression on the right-hand side of Eq. 45. Therefore Eq. 40 can be rewritten as the following equation.

$$\ddot{x} = -\sigma_c(0.01x + \dot{x}) \tag{46}$$

For an initial condition $x(0)$ the coefficient multiplying x can be chosen sufficiently small so that $|\dot{x}|$ decreases and then Eq. 46 reduces to

$$\ddot{x} + \dot{x} + 0.01x = 0 \tag{47}$$

from which it follows that $x \to 0$.

2.3.1 Simulation of the Proposed Control Algorithm 3

Figure 7 presents the evolution of x, y, θ and Fig. 8 presents the evolution of τ, f under the following initial conditions; $c = 0.1$, $\epsilon = 0.3$, $\dot{\theta}(0) = 0.5$, $\theta(0) = 0.1$, $\dot{y}(0) = 0.2$, $y(0) = 0.3$, $\dot{x}(0) = 0.1$, $x(0) = 0.4$, $y_d = 20$. As can be seen in Fig. 7 and 8, y converges to its desired value, θ and x converge both to zero, τ converges to zero and f converges to a constant value.

3 Results Analysis

Control algorithm 1 is based on a change of the input variables so that a linear control law can be defined to stabilize the altitude at a desired value. Subsequently it is assumed that the θ orientation is close to the origin. Then the model of the $x - \theta$ subsystem is reduced to a linear system that is controlled by a pole assignment control law. This control algorithm presents good behavior in numerical simulation,

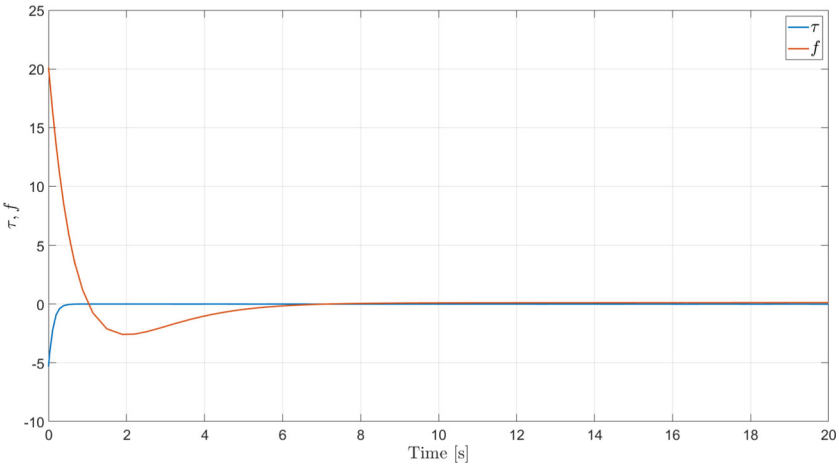

Fig. 6 Control inputs τ, f

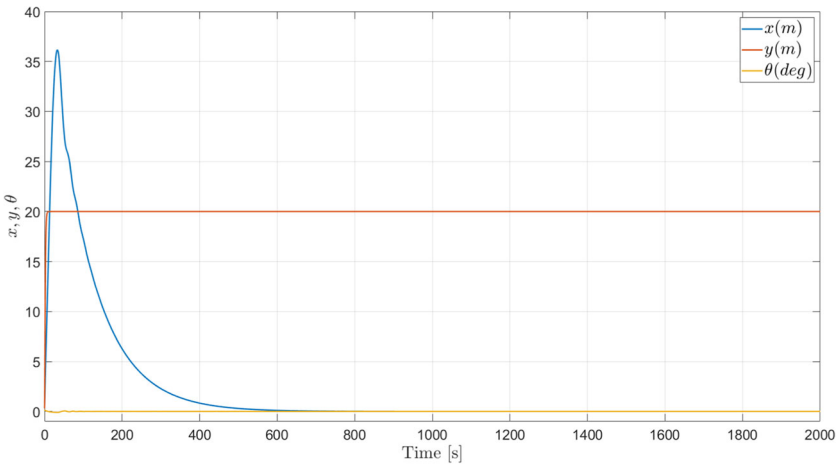

Fig. 7 Evolution of states x, y, θ

see Figs. 3 and 4. Note that in this case the control law for thrust and torque are linear. Control algorithm 1 was obtained assuming that the angular displacement θ was close to zero. Therefore the convergence to the origin of this controller is only local. Indeed, it has been observed in numerical simulations that if the initial position $x(0)$ is chosen far from the origin, then the controller will fail to stabilize the system. Since control algorithm 1 requires $|\theta(0)|$ to be small, one could propose a strategy that first makes θ small and then switch to control algorithm 1. However, control algorithms 2 and 3 do not require any switch. Notice from Table 1 that algorithm 1 provides the smallest values for rise time and settling time of x, y and θ.

Control algorithm 2, is based on the compensation of the nonlinearities in the altitude equation (y), so that the vehicle reaches a desired altitude. On the other hand, an orientation control law for θ in Eq. 36 is proposed so that θ converges to the sum of two saturation functions of x and $\dot{x}$. The saturation amplitudes a and b should be chosen small enough so that θ converges to a neighborhood of the origin. Furthermore, the amplitude of the saturation containing x, a, should be selected smaller that the amplitude of the saturation containing only $\dot{x}$, b. This is done so that the controller reduces first the size of the velocity $\dot{x}$ and once the velocity is smaller than b then equation Eq. 38 holds and it follows that both x and $\dot{x}$ converge to zero. However, Eq. 37 has been obtained assuming that θ is small and that τ is zero which is an approximation. This explains why x does not exactly converge to zero but oscilates in a neighbothood around the origin as can be seen is Fig. 5. This type of controller stabilizes the θ angle and ensures that x converges to a neighborhood of the origin. The selection of the values of the saturations amplitudes allows to vary the speed of convergence of the displacement to the origin, but also varies the amplitude of the oscillations of x.

Control algorithm 3, is similar to control algorithm 2 but in this case the torque control law contains a single saturation function. In this case too, the controller first reduces the horizontal velocity $\dot{x}$ and this is carried out by selecting a small weight 0.01 on the displacement x in Eq. 43. In this control algorithm it is also assumed that θ converges to a small neighborhood of the origin and that τ converges to zero which leads to Eq. 46 and finally Eq. 47. As can be seen in Figs. 7 and 8, the numerical simulations results using control

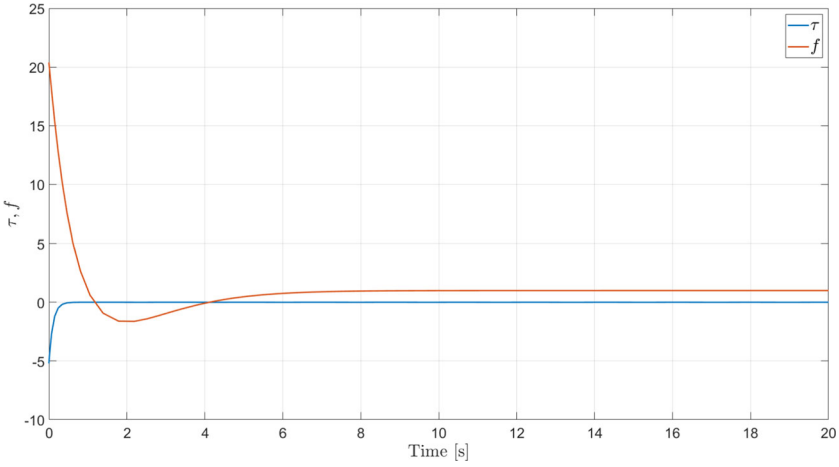

Fig. 8 Control inputs τ, f

algorithm 3 are better than those obtained with control algorithm 2. In this case the altitude converges also to its desired value but furthermore x and θ converge both to the origin.

4 Conclusions

In this paper a PVTOL with a steerable thruster was considered. The obtained dynamical model was a PVTOL with strong coupling at the inputs. To our knowledge, this type of system has not been studied in the literature. The objective was to control the evolution of this vehicle in the vertical plane. We proposed different control strategies to perform a stationary flight in the vertical plane. A closed-loop stability analysis and a comparison of the proposed methods in numerical simulation were performed. Future research includes developing a control strategy for tracking a predefined trajectory.

Acknowledgements The authors would like to thank the Center for Research and Advanced Studies (CINVESTAV) and the Council of Science and Technology (CONACYT) of Mexico for the support provided to carry out this research.

Author Contributions Authors Rogelio Lozano, Jhonatan F Eulopa - Hernandez and Sergio Rosario - Salazar contributed to the study conception and design. Material preparation, data collection and analysis were performed by all participants. All authors read and approved the final manuscript.

Funding This research was supported by the Center for Research and Advanced Studies (CINVESTAV) and the Council of Science and Technology (CONACYT) of Mexico.

Declarations

Consent for publication The authors affirm that they agree that this project be published.

Competing interests The authors have no relevant funding, employment, financial interests to disclose.

References

1. Hauser, J., Sastry, S., Meyer, G.: Nonlinear Control Design for Slightly Non-minimum Phase Systems: Application to V/STOL Aircraft *t **28**(4), 665–679 (1992)
2. Castillo, P., Dzul, A., Lozano, R.: Real-time stabilization and tracking of a four-rotor mini rotorcraft. IEEE Trans. Control Syst. Technol. **12**(4), 510–516 (2004). https://doi.org/10.1109/TCST.2004.825052
3. Brandão, A.S., Gandolfo, D., Sarcinelli-Filho, M., Carelli, R.: PVTOL maneuvers guided by a high-level nonlinear controller applied to a rotorcraft machine. Eur. J. Control. **20**(4), 172–179 (2014). https://doi.org/10.1016/j.ejcon.2014.04.003
4. Aguilar-Ibañez, C.: Stabilization of the PVTOL aircraft based on a sliding mode and a saturation function. Int. J. Robust Nonlinear Control **27**(5), 843–859 (2017). https://doi.org/10.1002/rnc.3601
5. Naldi, R., Furci, M., Sanfelice, R.G., Marconi, L.: Robust Global Trajectory Tracking for Underactuated VTOL Aerial Vehicles Using Inner-Outer Loop Control Paradigms. IEEE Trans. Autom. Control **62**(1), 97–112 (2017). https://doi.org/10.1109/TAC.2016.2557967
6. Tran, T.T., Ge, S.S., He, W.: Adaptive control of a quadrotor aerial vehicle with input constraints and uncertain parameters. Int. J. Control **91**(5), 1140–1160 (2018). https://doi.org/10.1080/00207179.2017.1309572
7. Aguilar-Ibanez, C., Sira-Ramirez, H., Suarez-Castanon, M.S., Garrido, R.: Robust Trajectory-Tracking Control of a PVTOL under Crosswind. Asian Journal of Control **21**(3), 1293–1306 (2019). https://doi.org/10.1002/asjc.1817
8. Lozano, R., Salazar, S., Flores, J.: Stabilization of the planar vertical take-off and landing using nonlinear feedback control. Int. J. Ro. Nonlinear Control **32** (2021) https://doi.org/10.1002/rnc.5808
9. Lozano, R., Salazar, S., Flores, D., González-Hernández, I.: PVTOL global stabilisation using a nested saturation control. Int. J. Control (2021). https://doi.org/10.1080/00207179.2021.1925348
10. Olfati-Saber, R.: Global configuration stabilization for the vtol aircraft with strong input coupling. Automatic Control, IEEE Transactions on **47**, 1949–1952 (2002). https://doi.org/10.1109/TAC.2002.804457
11. Notarstefano, G., Hauser, J.: Computing feasible trajectories for constrained maneuvering systems: the pvtol example. IFAC Proceedings Volumes **40** (2011) https://doi.org/10.3182/20070822-3-ZA-2920.00059
12. Dearing, T.L., Hauser, J., Chen, X., Nicotra, M.M., Petersen, C.: Efficient Trajectory Optimization for Constrained Spacecraft Attitude Maneuvers. J. Guid. Control. Dyn. **45**(4), 638–650 (2022). https://doi.org/10.2514/1.G006166

Rogelio Lozano was born in Monterrey, Mexico, in 1954. He received the B.S. degree in electronic engineering from the National Polytechnic Institute, Mexico City, Mexico, in 1975, the M.S. degree in electrical engineering from the Centro de Investigación y de Estudios Avanzados (CINVESTAV), Mexico City, in 1977, and the Ph.D. degree in automatic control from the Laboratoire d'Automatique de Grenoble, Grenoble, France, in 1981. From 1981 to 1989, he was with the Department of Electrical Engineering, CINVESTAV, where he was the Head of the Section of Automatic Control, from 1985 to 1987. He held visiting positions at The University of Newcastle, Australia, from 1983 to 1984, the NASA Langley Research Center, Langley, VA, USA, from 1987 to 1988, and the Laboratoire d'Automatique de Grenoble, from 1989 to 1990. He was promoted to first-class CNRS Research Director, in 1997. From 1995 to 2007, he was the Head of the Laboratory Heudiasyc, UMR 6599, CNRSUniversity of Technology of Compiègne (UTC), Compiègne, France. Since 1990, he has been the CNRS Research Director of UTC. He is currently the Head of the Laboratorio Franco-Mexicano de Informática y Automática Aplicada, UMI-CNRS, CINVESTAV. His current research interests include adaptive control of linear and nonlinear systems, robot manipulators, passive systems, teleoperation, and unmanned aerial vehicles. From 1987 to 2000, he was an Associate Editor of Automatica. He has been an Associate Editor of the International Journal of Adaptive Control and Signal Processing, since 1993.

Jhonatan F Eulopa-Hernandez received his B.S. in aeronautical engineering from National Polytechnic Institute (IPN), México, and M.S. degree in aerospace engineering from National Polytechnic Institute, México, in 2015 and 2018, respectively. He is currently Ph.D. student in Autonomous Air and Submarine Navigation Systems from Center for Research and Advanced Studies (CINVESTAV), México. His research interests include guidance and control for launch vehicle.

Sergio Salazar-Cruz was born in Tlaxcala, Mexico, in 1966. He received the B.S. degree in electronics engineering from the Benemérita Universidad Autónoma de Puebla, Puebla, Mexico, in 1992, the M.Sc. degree in electrical engineering from the Centro de Investigación y de Estudios Avanzados, Mexico City, Mexico, in 1995, and the Ph.D. degree in automatic control from the University of Technology of Compiègne (UTC), Compiègne, France, in 2005. Since 2008, he has been with the Laboratorio Franco-Mexicano de Informática y Automática Aplicada, Franco-Mexicano de Informática y Automática Aplicadas, Centre National de la Recherche Scientific, Centro de Investigación y de Estudios Avanzados. His current research interests include real-time control applications, embedded systems, unmanned aerial vehicles, and nonlinear dynamics and control.